

# Nucleic Acid Probes for Single-Molecule Localization Imaging of Cellular Biomolecules

Junyuan Wei,<sup>§</sup> Cailing Ji,<sup>§</sup> Yingfei Wang, Jie Tan,\* Quan Yuan,\* and Weihong Tan

Cite This: *Chem. Biomed. Imaging* 2023, 1, 18–29

Read Online

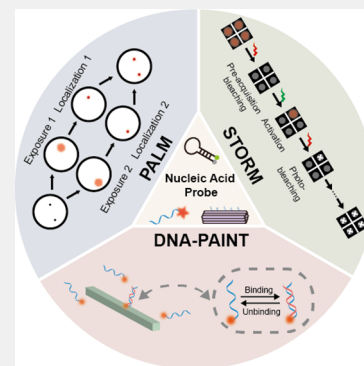
ACCESS |

Metrics & More

Article Recommendations

**ABSTRACT:** Endogenous biomolecules in cells are the basis of all life activities. Directly visualizing the structural characteristics and dynamic behaviors of cellular biomolecules is significant for understanding the molecular mechanisms in various biological processes. Single-molecule localization microscopy (SMLM) can circumvent the optical diffraction limit, achieving analysis of the fine structures and biological processes in living cells with nanoscale resolution. However, the large size of traditional imaging probes prevents SMLM from accurately locating fine structures and densely distributed biomolecules within cells. In recent years, nucleic acid probes have emerged as potential tools to replace conventional SMLM probes by virtue of their small size and high specificity. In addition, due to their programmability, nucleic acid probes with different conformations can be constructed via sequence design, further extending the application of SMLM in bioanalysis. Here, we discuss the design concepts of different conformational nucleic acid probes for SMLM and summarize the application of SMLM based on nucleic acid probes in the field of biomolecules. Furthermore, we provide a summary and future perspectives of the nucleic acid probe-based SMLM technology, aiming to provide guidance for the acquisition of nanoscale information about cellular biological processes.

**KEYWORDS:** single-molecule localization microscopy, super-resolution imaging, photoactivated localization microscopy, stochastic optical reconstruction microscopy, DNA-based point accumulation for imaging in nanoscale topography, intracellular molecular interaction, nucleic acid probes, conformational design, biomolecular analysis



## 1. INTRODUCTION

Visualizing organelle and endogenous biomolecules of living cells is conducive to study the relationship between their dynamics, structure, and function.<sup>1,2</sup> Subject to the diffraction limit, the resolution of conventional optical microscopy is usually greater than 200 nm, making it difficult to obtain the nanoscale structure and dynamics information in living cells.<sup>3,4</sup> Single-molecule localization microscopy (SMLM) randomly activates fluorescent molecules in batches so that only a few fluorescent molecules emit light in the imaging area at a time.<sup>5</sup> Subsequently, Gaussian fitting is used to localize the center position of the single fluorescent molecule (point diffusion function), thus cleverly bypassing the diffraction limit to achieve high-precision space localization.<sup>6</sup> Owing to their excellent photophysical properties, fluorescent proteins are often used as imaging probes for SMLM to obtain single-molecule localization information.<sup>7,8</sup> However, the larger size of these probes generally leads to significant steric hindrance interference, thereby reducing the localization precision.<sup>9</sup>

To improve the imaging effect of SMLM, the specificity and size of fluorescent probes are required to be optimized to achieve precise single-molecule localization. Nucleic acid probes not only possess excellent specific binding capability but also have much smaller sizes than traditional SMLM

probes such as fluorescent proteins.<sup>10,11</sup> Therefore, nucleic acid probes can effectively reduce steric hindrance and linkage errors, improving the localization precision.<sup>12</sup> In addition, due to their good programmable characteristics, nucleic acid probes can be modified controllably without changing their binding affinity and specificity.<sup>13</sup> By designing the nucleic acid sequences, multiple types of nucleic acid probes can be constructed according to different imaging conditions.<sup>14</sup> In summary, nucleic acid probes are promising probes for single-molecule imaging, further expanding the application of SMLM imaging.

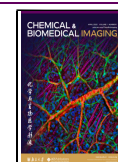
In recent years, based on the advantages of nucleic acid probes, various types of nucleic acid probes have been developed, such as DNA, RNA, PNA, and aptamers.<sup>13,15–17</sup> The development of these nucleic acid probes has greatly promoted the development of SMLM in biomedicine. However, there has not been a systematic discussion about

**Received:** January 14, 2023

**Revised:** March 4, 2023

**Accepted:** March 17, 2023

**Published:** April 14, 2023



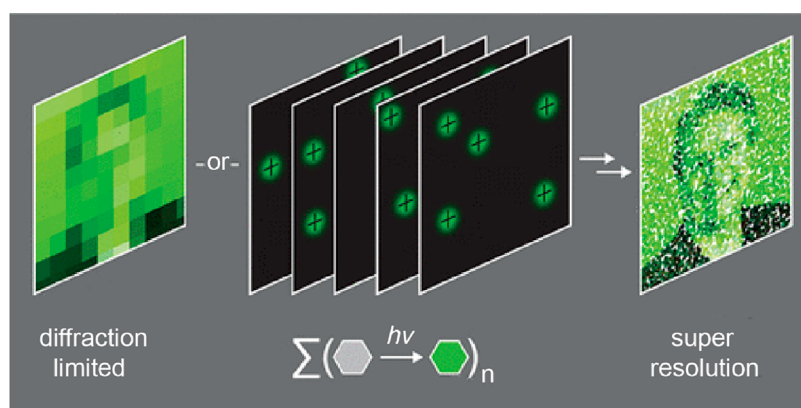


**Figure 1.** Principle of SMLM. In SMLM imaging, the process of “blinking–localization–reconstruction” is repeated to draw a super-resolution image. Reprinted with permission from ref 36. Copyright 2019, American Chemical Society.

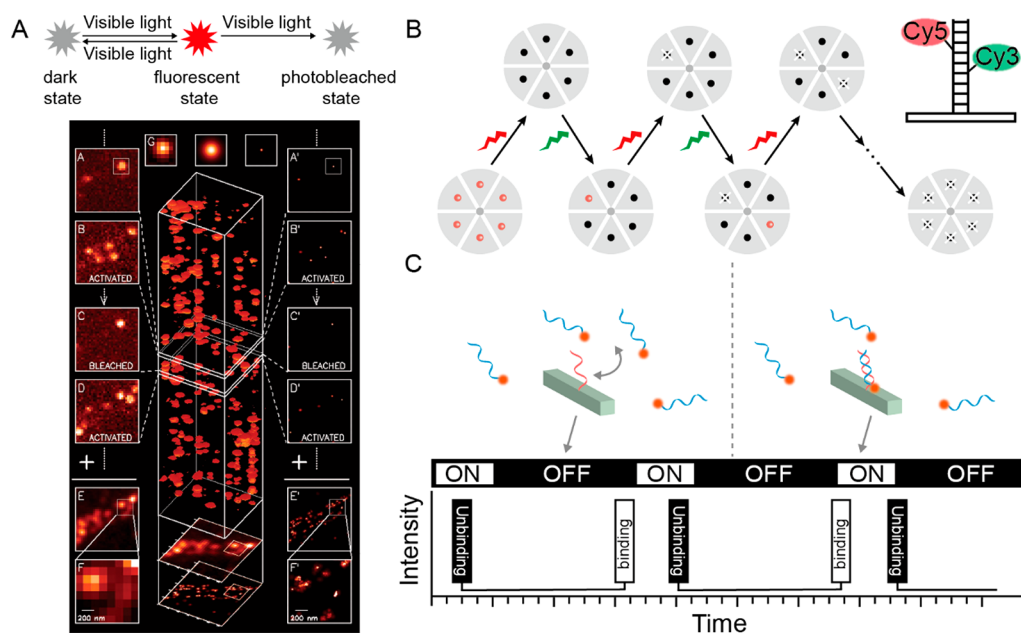


**Figure 2.** (A) Principles of PALM. The PA-FP molecules attach to proteins of interest. First, a 405 nm wavelength laser is used to excite them to fluorescent state, and then a 561 nm wavelength laser is used to stimulate fluorescence and eventually bleached. This process is repeated several times until all fluorescent molecules are bleached. Then, the collected fluorescent molecules are combined to locate and reconstruct the image. Reprinted with permission from ref 39. Copyright 2006, The American Association for the Advancement of Science. (B) Principles of STORM. In each imaging cycle, a green laser excites some fluorescent molecules to the fluorescent state, and then the red laser excites them to produce fluorescence until they enter the dark state. By repeating this cycle several times and integrating the precise positioning of the collected fluorescent molecules, super-resolution imaging can be achieved. (C) Principles of DNA-PAINT. Transient bonding occurs repeatedly between the imager probe labeled with fluorescent dyes and the docking strand coupled to the imaging object, thereby achieving the effect of “blinking”.

SMLM from the perspective of nucleic acid probe design. Here, we review the research progress of SMLM based on nucleic acid probes in this aspect. First, we introduce the principles of SMLM in detail. Then, the performance of nucleic acid probes with different conformations in SMLM is evaluated, and their application in biomolecular analysis is expounded. Finally, we discuss the challenges and future perspectives of SMLM based on nucleic acid probes, aiming to providing new ideas for future research in bioapplications.

## 2. PRINCIPLES OF SINGLE-MOLECULE LOCALIZATION MICROSCOPY

When a single-point light source passes through an optical imaging system, it will be affected by optical diffraction. This makes the resulting image a diffuse pattern rather than a point

of light.<sup>18,19</sup> This pattern consists of a bright center surrounded by a series of diffraction rings with waning brightness, called an Airy disk, also known as the point spread function (PSF).<sup>20,21</sup> As a result, when two imaging objects are close together in the scene, Airy patterns overlap together and cannot be distinguished.<sup>22,23</sup> According to the Rayleigh criterion, it is just possible to distinguish the image formed by two points when the center of one Airy disk overlaps with the first-order dark ring of another Airy disk. At this time, the distance between the center of the two Airy patterns is equal to the radius of the Airy disk.<sup>24</sup> Calculating the distance between the corresponding two Airy patterns, that is, the resolution limit, is summarized by the equation<sup>24,25</sup>

$$d = 0.61\lambda/NA$$

where  $\lambda$  is the wavelength of light and NA is the numerical aperture of the microscope objective lens.<sup>26</sup> From this point of view, the microscope resolution is related only to the wavelength of incident light and the numerical aperture of the microscope objective lens.<sup>27</sup> Therefore, limited by the objective lens, traditional optical microscopes cannot break through the optical resolution limit when imaging densely distributed light spots, making it difficult to achieve high-resolution imaging.<sup>28,29</sup>

SMLM can overcome the diffraction-limited resolution barrier of optical microscopy, achieving super resolution imaging.<sup>30</sup> As shown in Figure 1, the core ideas of SMLM are “blinking”, “localization,” and “reconstruction”.<sup>5</sup> The “blinking” is usually based on specific fluorescent probes.<sup>31</sup> By controlling the laser intensity, only a sparsely distributed small number of fluorescent molecules in the imaging area are activated at a time.<sup>1,32</sup> Then, an imaging system is used to record images of a small number of fluorescent molecules randomly activated multiple times.<sup>33</sup> “Localization” refers to the determination of the precise position of the fluorescent molecule using a single-molecule localization algorithm (e.g., Gaussian fitting).<sup>34,35</sup> The “reconstruction” involves superimposing a series of collected images that cover the precise positioning information on fluorescent molecules, resulting in a complete super-resolution image.<sup>36</sup>

At present, SMLM techniques mainly include three types: photoactivated localization microscopy (PALM), stochastic optical reconstruction microscopy (STORM), and DNA-based point accumulation for imaging in nanoscale topography (DNA-PAINT).<sup>37</sup> Among them, the principles of PALM and STORM are basically the same, but the fluorescent labels used are different.<sup>38</sup> PALM was first proposed by Eric Betzig and Harald Hess in 2006.<sup>39</sup> The photoactivate protein PA-GFP, a mutant of GFP fluorescent protein, is used as a fluorescent tag to label the target protein in this technique. PA-GFP is a kind of photoactivate protein that can change from a low-fluorescence state to a high-fluorescence state when activated with light of a particular wavelength (405 nm). In PALM imaging, 405 nm wavelength laser is first used to irradiate the cell surface with low energy to activate several sparsely distributed fluorescent proteins, and then a 488 nm wavelength laser is used to stimulate fluorescence. Then it is precisely positioned by Gaussian fitting, and the fluorescent proteins that have been positioned correctly continued to be irradiated with 488 nm wavelength laser for a long time. Precise localization of a large number of fluorescent proteins can be achieved by repeating the “activation–excitation–localization–bleaching” process many times.<sup>40</sup> Merging these fluorescent images of these proteins can finally reconstruct an image with a resolution more than 10 times higher than that of a traditional optical microscope (Figure 2A).<sup>41,42</sup>

Although the super-resolution visualization of cellular foreign proteins can be achieved using PALM, the imaging of intracellular proteins cannot be done. STORM has been developed to solve this problem.<sup>30</sup> As illustrated in Figure 2B, Cy3–Cy5 dye pairs are used to label endogenous proteins in this technique.<sup>43</sup> The photoswitch of Cy5 can be realized by switching between the 633 nm wavelength laser and the 532 nm wavelength laser. Specifically, the sample is continuously irradiated by a 633 nm wavelength laser to keep Cy5 in a luminous state, but long-term irradiation with a high-intensity laser will cause all Cy5 molecules to quickly change from a fluorescent state to a dark state. At this time, a low-intensity

laser with wavelength of 532 nm is used to excite Cy3. Fluorescence resonance energy transfer (FRET) occurs between Cy3 and Cy5, making a few randomly distributed Cy5 molecules activated in a fluorescent state. After that, under the excitation of 633 nm wavelength red light, the Cy5 molecules in the fluorescent state emit fluorescence and eventually switch to the dark state. By cycling this process multiple times until most of the fluorescent molecules have been bleached, high-resolution images of endogenous proteins can be obtained with imaging resolution up to 20 nm. However, the design of this fluorescent label is not conducive to the extensive use of STORM. In 2008, Heilemann’s team found that some cyanine dyes could directly convert the dark state to the fluorescent state through two laser beams of different wavelengths without the assistance of other fluorescent molecules, such as Alexa Fluor 647 (AF647).<sup>44</sup> This technique is more direct to use and is called direct STORM (dSTORM). At first, a 647 nm wavelength laser is used to irradiate the fluorescent dye to make it enter the dark state. A laser with wavelength of 514 nm is then used to excite the dye, making it return to the fluorescent state. dSTORM technology avoids complex fluorescent molecular design, thereby reducing the threshold for the application.

DNA-PAINT is a newer technique than PALM and STORM.<sup>45</sup> This technology was improved by Joerg Schnitzbauer et al. based on PAINT technology. PAINT technology is a method for subdiffraction imaging that accumulates points by collisional flux.<sup>46</sup> In PAINT imaging, the imaging target is continuously targeted by fluorescent probes in the solution. When fluorescent probes bind to the target, a significant fluorescent signal will appear. Therefore, using an unlimited number of fluorescent probes to target the object, a complete image of the object can be obtained. Based on this, DNA-PAINT introduces strands of DNA, and the technique works by exploiting the complementarity of DNA strands to produce an effect similar to the “blinking” of fluorescent molecules.<sup>47</sup> In DNA-PAINT, one strand of the DNA double helix is used to bind to the target as a “docking strand”, while the other strand binds to fluorescent molecules as an “imager probe”. During imaging, the docking strand will repeatedly associate and dissociate with the imager probe (Figure 2C). The optimal blinking rate can be determined by adjusting the binding intensity and DNA concentration. Afterward, the resulting data are located and reconstructed to obtain the final super-resolution image.

### 3. PERFORMANCE EVALUATION OF DIFFERENT NUCLEIC ACID PROBES FOR SMLM

Nucleic acid probes exhibit comparable or stronger specificity and affinity than traditional photoaffinity probes, such as fluorescent proteins. Moreover, the small size of nucleic acid probes can minimize steric hindrance and linkage error, significantly improving the localization precision and image quality of SMLM.<sup>48</sup> In addition, owing to the excellent programmable characteristics, nucleic acid probes with various conformations can be constructed by sequence design, thereby regulating the fluorescence intensity and blinking time of the fluorescent probes.<sup>49,50</sup> This undoubtedly further expands the application of nucleic acid probes in SMLM imaging. In this section, we will discuss the construction methods and imaging properties of nucleic acid probes with different conformations for SMLM.

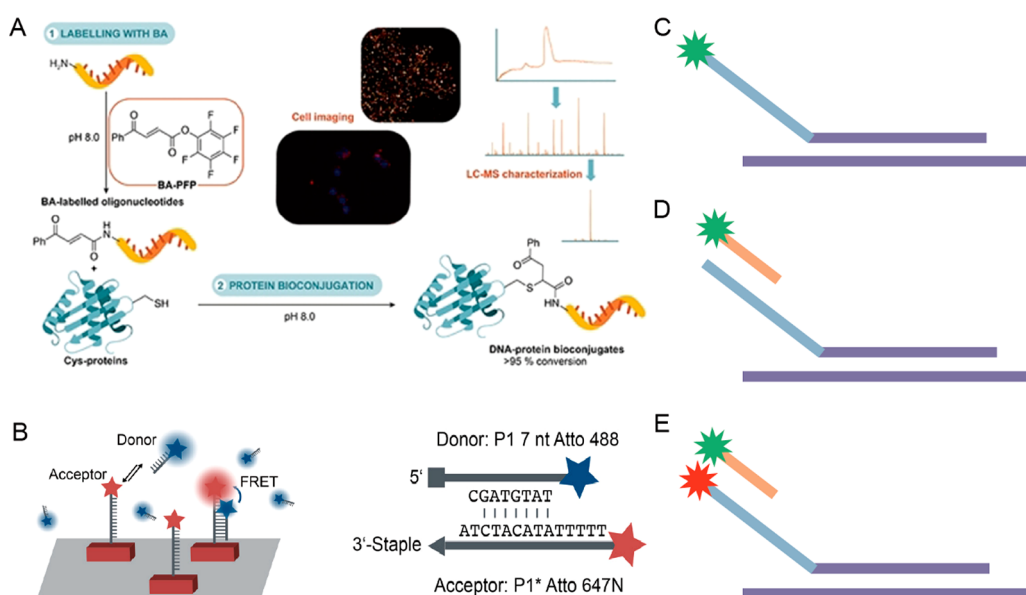


**Figure 3.** (A) Schematic diagram of constructing linear nucleic acid probes for super-resolution imaging of HER2. Reprinted with permission from ref 53. Copyright 2021, The Authors. *Angewandte Chemie International Edition* published by Wiley-VCH GmbH. (B) Working principle of linear nucleic acid probes based on FRET for DNA-PAINT imaging. Reprinted with permission from ref 57. Copyright 2017, American Chemical Society. (C) Three main methods for constructing STORM imaging probes based on the Oligopaint for accurately locating the target genome.

### 3.1. Linear Nucleic Acid Probes for SMLM

Linear nucleic acid probes are the most traditional nucleic acid probes used in SMLM imaging.<sup>51,52</sup> Such probes usually only need to be coupled with fluorophores on the nucleic acid strands, showing the advantages of simple synthesis and facile modification. When synergizing with SMLM technology, the construction strategies of linear nucleic acid probes have a large impact on the imaging performance. Therefore, it is particularly important to rationally construct linear nucleic acid probes to pursue remarkable imaging resolution.

As one of the most widely used SMLM technologies, DNA-PAINT exploits the dynamic binding and unbinding properties of DNA oligonucleotide strands to achieve the “blinking” effect that is similar to STORM and PALM microimaging techniques. Typically, one of the double-stranded DNA serves as a docking strand that binds to the target, while the other complementary oligonucleotide strand is modified with fluorescent dyes as the imager strand.<sup>47</sup> This allows linear nucleic acid probes to develop rapidly in SMLM imaging. For example, Konč’s group coupled oligonucleotide SS11 with an antibody targeting HER2 as a docking strand, whereas a complementary strand of DNA labeled with a fluorescent molecule served as an imager strand (Figure 3A).<sup>53</sup> The super-resolution images of HER2 were obtained via repeated combination and separation of docking strands and imager strands. However, when linear nucleic acid probes are used for imaging, unbound imager probes in solution will generate high background fluorescence, significantly affecting the image quality. This problem is usually avoided by limiting the probe concentration and reducing the illumination intensity. However, the low probe concentration and light intensity result in a few fluorescence “blinking” events of each image acquisition.<sup>54,55</sup> In recent years, researchers have found that linear DNA probes based on fluorescence resonance energy transfer (FRET) can address this matter.<sup>56</sup> Auer et al. connected a donor dye Atto 488 and an acceptor dye Atto 647N to imager probes and docking strands, respectively

(Figure 3B).<sup>57</sup> Under 488 nm irradiation, the energy of Atto 488 was transferred to acceptor Atto 647N and then lit up Atto 647N fluorescent. In this method, the large shift between the excitation wavelength of donor and acceptor dyes prevents the receptor dyes from being directly excited by the laser, effectively avoiding background fluorescence during imaging. Thus, FRET-based imager probes can achieve super-resolution imaging. However, the simultaneous binding of imager probes and docking strands to the same target at the same time is random, resulting in the short luminescence duration and increased data acquisition time. Therefore, although FRET technology is an improvement over traditional methods, it still cannot meet the needs of existing applications. To simultaneously meet the low background fluorescence and fast binding dynamics, Chung et al. further designed and developed a novel single-stranded-linear nucleic acid probe, including self-quenching imager strands and partially mismatched docking strands.<sup>55</sup> The fluorophore and the quencher were conjugated at both ends of an oligonucleotide strand with a length of 15bp to construct the imager probe. The structural flexibility of the oligonucleotide strand allows the fluorophore and quencher to be in close proximity and causes strong quenching. When combined with the docking strand, the resulting rigid double helix structure spatially separated the fluorophore from the quencher, thereby restoring fluorescence. Some mismatched bases were introduced into the docking strand, so that the length of the pairing region between the imager probe and the docking strand was 10 bp to meet the requirement of fast imaging. The introduction of mismatched bases effectively realized super-resolution high-speed imaging without affecting the normal luminescence of the fluorophore (pairing region  $\geq 15$  base pairs), shortening the imaging time.

With the rapid development of nucleic acid probes, linear nucleic acid probes are also gradually used for STORM and PALM imaging. Beliveau et al. constructed an oligonucleotide probe for targeting the genome and called it Oligopaints.<sup>58</sup> Oligopaints are short single-stranded oligonucleotides, con-

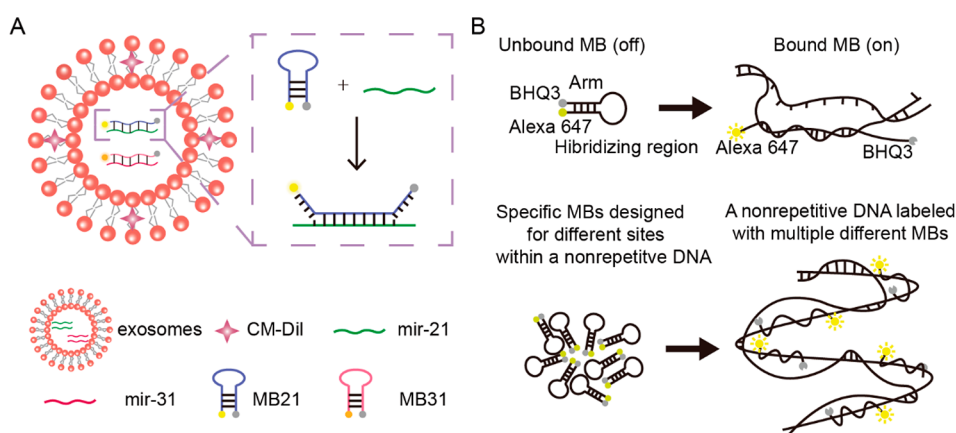


**Figure 4.** (A) Working principle of the hairpin nucleic acid probes used for super-resolution imaging of exosomal miRNAs. (B) Schematic diagram of genome imaging by STORM technique using hairpin nucleic acid probes modified with Alexa-647 and BHQ3.

sisting of genomic homologous short sequences and non-genomic sequences linked on the side (known as Mainstreet). In the presence of genomic targets, genome homologous regions in the Oligopaints were able to hybridize with genomic targets. In contrast, the Mainstreets always remained single-stranded, giving Oligopaints the ability to act as single-molecule imaging probes. High-resolution *in situ* visualization of genome sequences is essential for understanding loop interactions and chromatin organization in single cell. Based on this, the authors achieved super-resolution imaging of the fine-scale genomic structure based on Oligopaints and STORM imaging techniques. In general, there were three main methods that constructed STORM imaging probes based on the Oligopaints for accurately locating the target genome. One of the simplest methods was to directly couple fluorescent molecules on Oligopaints that can switch the optical switching state, such as Cy5 and AF647 (Figure 3C). After the laser excitation, Oligopaints transformed the optical switching state to achieve the effect of “blinking”. Another method was similar; the difference was that this method did not directly connect the fluorophore to the Oligopaints. Instead, a new oligonucleotide strand was built to connect with the fluorophore and then hybridized to Mainstreets of the Oligopaint (Figure 3D). Subsequently, the conversion between the fluorescent state and the dark state was also completed by laser regulation. The last method was based on the FRET strategy, where the receptor fluorophores were coupled to the Oligopaints. Whereas the donor fluorophores were connected to another oligonucleotide strand to hybridize with Mainstreet in the Oligopaints (Figure 3E).<sup>51</sup> Additionally, Xie et al. constructed linear fluorescent nucleic acid probes based on the transposon enzyme recombination technique for PALM imaging, realizing the visualization of the genome on the nanometer scale.<sup>52</sup> Specifically, Tn5 transposase was linked to the photoactivated fluorescent dye Janelia Fluor 549 on DNA oligonucleotides containing the mosaic ends of the Tn5 transposon. After that, a transposon enzyme recombination technique was used to form active transposon complexes *in vitro*, thereby constructing fluorescent probes.

### 3.2. Hairpin Nucleic Acid Probes for SMLM

Hairpin-shaped nucleic acids are nucleic acid molecules with a stem-loop structure formed by complementary base pairing inside single-stranded nucleic acids.<sup>59</sup> This type of structure is shaped like a hairpin in a stable state, but under certain

conditions, the stem in the stem-loop structure can be opened. Based on the particularity of this structure, hairpin-shaped nucleic acids are widely used in the construction of SMLM imaging probes. As originally designed, a hairpin nucleic acid probe contains a sequence complementary to the target, and the probe is flanked by self-complementary termini and carries a fluorophore and a quencher at the 3'- and 5'-ends. In the absence of the targets, these hairpin-shaped nucleic acids maintain closed stem-loop structures in which the fluorophore and quencher are in close proximity. The fluorescence emitted by the fluorophores is absorbed by quenchers via FRET, resulting in no apparent fluorescent signal. However, the interaction between nucleic acid probes and targets leads to the closed stem-loop structure being opened when targets are present. Once fluorophores and quenchers are spatially separated, the fluorescence increases.<sup>60</sup> Accordingly, hairpin-shaped nucleic acid probes can effectively avoid the interference of background fluorescence and realize target-specific imaging, presenting a powerful choice to increase the resolution of SMLM imaging. In addition, the use of fluorophore modification with different excitation and emission wavelengths can extend hairpin nucleic acid probes for simultaneous multicolor imaging, further promoting the application of SMLM in life sciences.

Based on their unique luminescence advantages, hairpin-shaped nucleic acid probes can accurately locate nucleic acids via nucleic acid hybridization. Additionally, the utilization of fluorescent dyes with different excitation wavelengths to modify hairpin-shaped nucleic acid probes allows simultaneous imaging of multiple key nucleic acid molecules in the physiological environment. Therefore, hairpin-shaped nucleic acid probes can be used as potential tools for exploring the physiological functions of nucleic acid molecules in complex environments. For instance, exosomal miRNAs, small non-coding RNA molecules secreted by cancer-associated fibrocytes, normal fibrocytes, and cancer cells, are able to regulate tumorigenesis and metastasis.<sup>61,62</sup> To better analyze the structure of exosomal miRNAs and explore their role in tumor metastasis, Chen et al. designed and developed hairpin nucleic acid probes for SMLM imaging of exosomal miRNAs. More specifically, two hairpin nucleic acid probes MB21 and MB31 were constructed for exosomal mir-21 and mir-31.<sup>63</sup> As illustrated in Figure 4A, both ends of MB21 are modified by fluorophore Cy5 and black hole quencher 3 (BHQ3); both ends of MB31 are modified by fluorophore AF488 and black

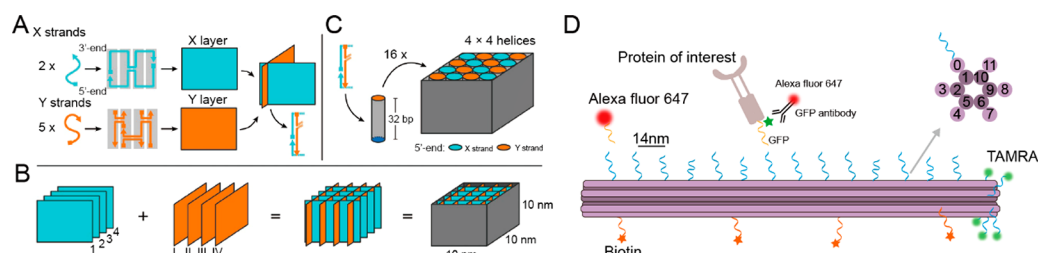


**Figure 5.** (A–C) Schematic diagram of the construction of DNA cubes. Each two X strands (blue) formed an X layer, and each five Y strands (orange) formed a Y layer. Four parallel X layers and four Y layers perpendicular to the X layer were assembled orthogonally to form a cube structure. Reprinted with permission from ref 70. Copyright 2015, Wiley-VCH Verlag GmbH & Co. KGaA. (D) Principle of STORM imaging of proteins using DNA origami structure as probes.

hole quencher 1 (BHQ1). Among them, the excitation wavelengths of Cy5 and AF488 were 650 and 488 nm, respectively. The difference in wavelength thus effectively avoids the fluorescence crosstalk during the imaging process, achieving the dual-color imaging of mir-21 and mir-31. In 2015, fluorescence in situ hybridization (FISH) was developed to enable targeted imaging of the genome.<sup>58</sup> However, fluorescent-labeled FISH probes will generate massive amounts of nonspecific fluorescence, limiting the further development of FISH technology. In view of this, Ni's team designed hairpin-structure FISH probes that combined with three-dimensional (3D) STORM technology to visualize the 2.5 kb nonrepetitive DNA in human or mouse genomes.<sup>64</sup> The authors designed nucleic acid molecules containing a pairing region composed of 42 nucleotides that hybridized with the target sequence and modified with fluorophore Alexa-647 and BHQ3 at the terminals. In the presence of target genes, the paired region in the hairpin-shaped probe hybridized with them, unlocking the hairpin secondary structure. The fluorophore Alexa-647 spatially separated from BHQ3 to resume the strong fluorescence. Consequently, the 3D fine nanostructures of endogenous DNA were observed under 3D-STORM (Figure 4B).

As another important biomacromolecule in organisms, visual detection of the spatial distribution and dynamics of cellular key proteins is significant for understanding their biological functions and molecular behaviors. In recent years, researchers have also focused on developing hairpin nucleic acid probes for SMLM imaging of proteins under physiological conditions. Pereira's team designed hairpin nucleic acid probes with a loop region consisting of 9 mer polythymidine linker.<sup>65</sup> These thymine bases are biotinylated, enabling probes to bind to streptavidin-conjugated labeling agents for targeting target proteins. An ATTO550 fluorophore and a Black Hole Quencher 2 (BHQ2) were conjugated on the 5' end and 3' end of nucleic acid probes, respectively. Due to the excellent photoswitching properties of these hairpin-shaped nucleic acid probes, the super-resolution imaging of  $\beta$ -tubulin in cells was realized by the STORM technique.

### 3.3. Polyhedral Nucleic Acid Probes for SMLM

As natural biological macromolecules, nucleic acids have unique properties, such as excellent biocompatibility and molecular programmability.<sup>66</sup> These unique properties, combined with highly predictable Watson–Crick base-pairing rules at the nanoscale, make nucleic acid molecules natural candidates for constructing polyhedral nanostructures.<sup>13,50</sup> With precise design and appropriate construction strategies, nucleic acid molecules can be assembled to form polyhedral

nucleic acid probes of specific sizes and shapes.<sup>14,67</sup> These nucleic acid probes possess accurate addressability and spatial orientation, further enhancing the imaging sensitivity and accuracy of SMLM in the complex biological environment.<sup>68,69</sup> Therefore, the SMLM technique based on polygonal nucleic acid probes can qualitatively analyze cellular biomolecules with a high temporal and spatial resolution, contributing to the study of the structure and function of biomolecules in cells at the single-molecule level.

Scheible et al. designed cube-shaped nucleic acid probes for DNA-PAINT imaging.<sup>70</sup> Based on the “DNA brick” strategy, two sets of linear DNA oligonucleotide chains with different lengths were utilized to construct a small DNA cube with a side length of only 10 nm. In the hybrid assembly strategy, the longer oligonucleotides were regarded as the X strands, whereas the shorter oligonucleotides serve as the Y strands. As shown in Figure 5A, each two X strands formed an X layer, and each five Y strands formed a Y layer. Four parallel X layers and four Y layers perpendicular to the X layer were assembled orthogonally to form a cube structure (Figure 5B). As a result, the cube consisted of  $4 \times 4$  parallel double helices, each helix with a height of 32 base pairs (bp) (Figure 5C). In order to explore the super-resolution imaging capabilities of these cube nucleic acid probes, DNA filaments were constructed as targets. Eventually, a clear copositioning image of the two structures could be obtained using DNA-PAINT based on DNA cubes.

By hybridizing long single-stranded scaffold DNA with a series of designed short DNA fragments, DNA origami technology can controllably construct nanopatterns or structures of different shapes and conformations.<sup>68</sup> Fluorophores can be further modified on the DNA origami structure at a specified position and spatial distance via the sequence design, endowing them with the ability to serve as multifunctional SMLM imaging probes. Lin's team designed a new geometrically encoded fluorescent barcode based on the DNA origami technology, extending the nucleic acid probe-based SMLM technology to multicolor imaging.<sup>71</sup> The author first assembled six-helix bundle DNA nanorods that were  $\sim 800$  nm long. Four symmetrically arranged zones were then selected to couple three dyes with different spectra (Atto488, Cy3b, and Atto655) to construct multiple fluorescent barcodes. The neighboring zones were separated by 113 nm, well below the diffraction limit. The imaging results showed that the DNA nanoprobe can realize three-color DNA-PAINT imaging. Owing to their excellent fluorescence coding ability, polyhedral nucleic acid probes are expected to be used for imaging a variety of nanoscale structures in cells, providing comprehensive molecular structure and behavior information. Zanacchi's

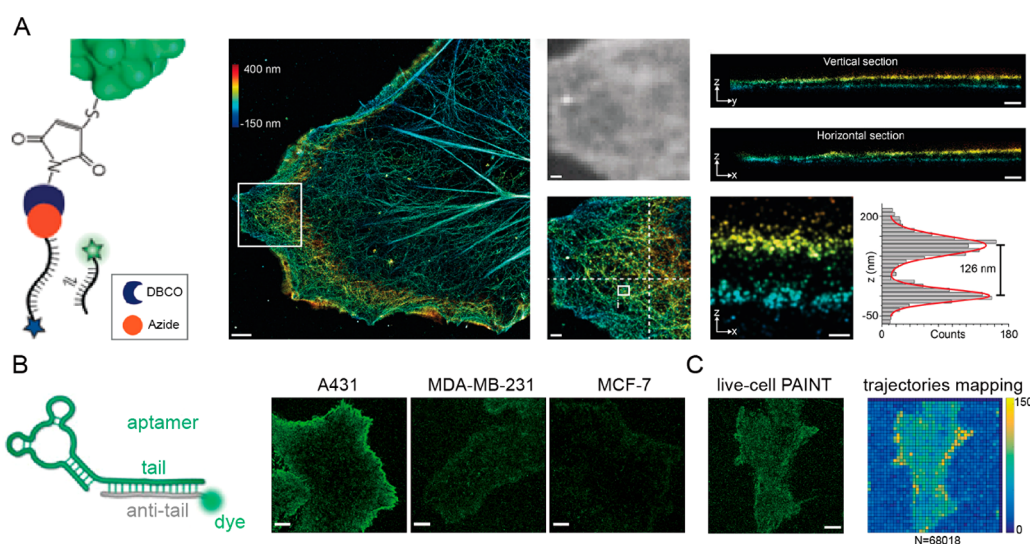


**Figure 6.** (A) DNA-PAINT technology with linear nucleic acid probes for imaging the dual-layer organization of actin in COS-7 cells. Cross-sectional histogram analysis showed that the distance between two actin layers is about 130 nm in a single cell. Reprinted with permission from ref 78. Copyright 2018, Wiley-VCH Verlag GmbH & Co. KGaA. (B) PAINT imaging of three cell lines with different EGFR expression levels. The signal intensities were positively correlated with cell EGFR expression. Reprinted with permission from ref 82. Copyright 2020, The Authors. Published by Wiley-VCH GmbH. (C) Reconstructed PAINT image and density map of trajectories of EGFR on MDA-MB-231 cells. Reprinted with permission from ref 82. Copyright 2020, The Authors. Published by Wiley-VCH GmbH.

team combined 3D DNA origami structures with GFP antibodies to build polyhedral nucleic acid probes, cooperating with the STORM technique and mapping specific cellular proteins.<sup>72</sup> As illustrated in the design idea in Figure 5D, 3D DNA origami structures were used as the chassis, and the protruding handle sequences around the chassis can provide site- and sequence-specific attachment points for single fluorophores or for protein of interest. Fluorophores TAMRA attached at the terminal of origami structures were used to identify the chassis. The complementary antihandle sequences were designed to couple with the protein of interest containing GFP and bind to the nucleic acid polyhedral structures. The GFP on the protein of interest was then labeled by primary anti-GFP antibodies and photoswitchable dye pair (AF405–AF647) labeled secondary antibodies. Consequently, STORM imaging was performed to achieve clustering analysis of the target proteins.

#### 4. SMLM APPLICATION BASED ON NUCLEIC ACID PROBES

Currently, SMLM is the highest-resolution super-resolution microscopic imaging technology, enabling precise localization of individual molecules.<sup>73</sup> Nucleic acid probes have irreplaceable advantages of traditional fluorescent probes, such as high targeting and small size.<sup>16,74</sup> Therefore, nucleic acid probe-based SMLM can provide more abundant and detailed information to reveal the life processes in biological systems. The following section elaborates on the application of SMLM based on nucleic acid probes in biological analysis.

##### 4.1. Explore the Spatial Distribution of Intracellular Biomolecules

Vital cellular biomolecules, including nucleic acids, proteins, lipids, can participate in regulating a series of biological processes to complete complex life activities.<sup>75</sup> The abnormal changes in the location, content or structure of these key biomolecules are supposed to mediate the occurrence and development of many diseases.<sup>76</sup> Therefore, visualizing intra-

cellular biomolecules is of great significance for understanding complex cellular behaviors and life processes. However, biomolecules in cells are usually small in size and densely distributed, making them difficult to image them at high resolution with traditional fluorescence microscopy.<sup>22</sup> The SMLM technique based on nucleic acid probes can break the optical diffraction limit, thereby analyzing the intracellular distribution of key biomolecules at the single-molecule level.<sup>77</sup>

Schlichthaerle and colleagues constructed linear DNA probes coupled with Affimers reagents.<sup>78</sup> As an antibody-like labeling group, the modification of the Affimers reagent endows these probes with excellent actin-specific binding ability and stable imaging capability. Visualization of actin in COS-7 cells in three-dimensional space was achieved using DNA-PAINT based on these linear probes. The distribution of two different actin layers in the cell was shown in Figure 6A. The apparent thickness of these actin layers was around 40 nm, and the distance between two actin layers was approximately 130 nm. In addition to imaging proteins, SMLM can also be applied to analyze other biological molecules. Exosomes are a kind of nanovesicle secreted by a variety of cells and can deliver biologically active macromolecules such as proteins, nucleic acids, and lipids.<sup>79</sup> Reportedly, exosomes are especially rich in miRNAs that are small noncoding RNA molecules, playing an important role in cell development, proliferation and apoptosis.<sup>62,80</sup> Recently, researchers have found that certain exosomal miRNAs can be released from the exosome and are major players for the absorption of exosomes by receptor cells.<sup>81</sup> Therefore, real-time tracking of exosomal miRNAs is essential for understanding the biological functions of exosomes. Chen et al. designed hairpin nucleic acid probes to target exosomal mir-21.<sup>63</sup> A fluorophore, Cy5, and a quencher, BHQ3, were terminally labeled at the stem ends. Moreover, exosome membranes were labeled with a green fluorescent dye, CM-DiI. Then, dual-color PALM imaging was performed to explore the release process of exosomal mir-21 in receptor cells. Due to the limitation of the photoswitching

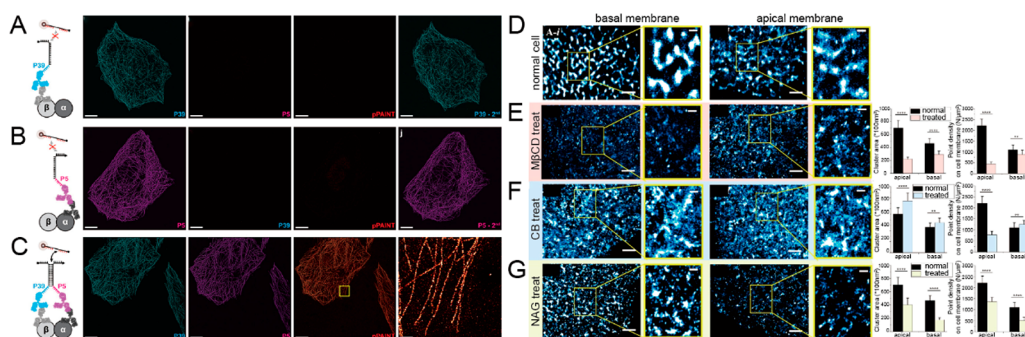


**Figure 7.** (A and B) Proximity-PAINT imaging of the interaction between  $\alpha$ - and  $\beta$ -Tubulin with a single docking strand. Reprinted with permission from ref 91. Copyright 2020, The Authors. Published by Wiley-VCH GmbH. (C) Proximity-PAINT imaging of the interaction between  $\alpha$ - and  $\beta$ -Tubulin with two docking strands. Reprinted with permission from ref 91. Copyright 2020, The Authors. Published by Wiley-VCH GmbH. (D–G) The effect of lipid raft, actin cytoskeleton, or carbohydrate chains on the interactions between PTK7 proteins distributed in the MCF10A basal or apical membranes. Reprinted with permission from ref 92. Copyright 2021, American Chemical Society.

speed, the maximum acquisition frequency of the PALM was 31.25 Hz. In addition, the super-resolution microscopic image of each fluorescence channel required 100 frames to be reconstructed, with a time resolution of about 6.4 s. At the beginning of imaging, the fluorescence of exosomes and exosomal mir-21 basically overlapped, and the maximum distance between the fluorescence center of exosome and exosomal mir-21 was about 20 nm. Gradually, a distinct separation of the fluorescence overlaps between exosome and exosomal mir-21 was observed using dual-color PALM imaging. After approximately 40 s, mir-21 disappeared from view, while the exosome remained *in situ*. In conclusion, SMLM based on nucleic acid probes can not only visualize intracellular biomolecules but also analyze their dynamic distribution process.

With the explosive development of imaging techniques, SMLM can be further applied in biomedicine and become an emerging tool for disease treatment. Biomarkers are indicators for objective detection and evaluation of various physiological and pathological processes. Biomarkers are indicators of objective detection and evaluation of normal biological processes, pathological processes, and pharmacological responses to therapeutic interventions. Changes in the content and distribution of cellular biomarkers are closely related to the occurrence, development, and prognosis of diseases.<sup>76</sup> Therefore, accurately identifying the distribution patterns and content of biomarkers are practically important for disease diagnosis, drug development, and clinical treatment. Epidermal growth factor receptor (EGFR) is one of the members of the epidermal growth factor receptor family. Studies have shown that EGFR is closely related to the proliferation, angiogenesis, tumor invasion, and metastasis of tumor cells. At present, overexpression of EGFR has been found in many solid tumors. Delcanale et al. constructed linear nucleic acid probes using a variant of Min E07 aptamer that was conjugated with Atto647N fluorescent dye.<sup>82</sup> Combined with PAINT imaging, these linear nucleic acid probes were utilized to spatially visualize three cell lines with different EGFR expression: MDA-MB-231 cell line (moderate EGFR levels), MCF-7 cell line (very low EGFR levels), and A431 cell (high EGFR levels). Distinct differences in fluorescence signals were observed, as shown in Figure 6B. The signal intensities were positively correlated with cell EGFR expression. Furthermore, a density map of trajectory distributions on the whole cell membrane area was calculated by binning the mass center of each

trajectory with an arbitrary pixel size. Specific subpopulations of molecules could eventually be mapped on the cell surface (Figure 6C). Therefore, SMLM based on nucleic acid probes can monitor changes in the distribution of disease markers. This is especially helpful to explore the molecular mechanism of disease occurrence and development.

#### 4.2. Detection of Intracellular Molecular Interactions

The interaction between biomolecules in cells controls cell behaviors and functions, becoming the structural foundation of all life activities.<sup>83</sup> Therefore, elucidating the interactions between intracellular biomolecules at the molecular level is crucial for gaining insight into the detailed mechanisms of cellular activities. At present, the traditional assays for analyzing molecular interaction mainly include surface plasmon resonance, isothermal titration calorimetry, electrophoretic mobility shift assays, and fluorescence spectrometry.<sup>84–87</sup> However, these methods can only reflect the behavior of biomolecule clusters and cannot study the interactions between individual molecules. Nucleic acid probe-based SMLM allows visual monitoring of dynamic interaction processes between biomolecules at the nanoscale. Based on this, researchers can better understand and regulate key biomolecular-mediated life processes, promoting the development of life sciences.

EGFR receptors become activated by homo- or heterodimerization of the receptors after epidermal growth factor (EGF) binding.<sup>88</sup> Dimerization of receptors can further activate a series of downstream signaling pathways that regulate numerous biological processes including cellular proliferation, apoptosis, and tumor progression.<sup>89</sup> Therefore, precise visualization of the interaction between EGF and EGFR can not only contribute to understanding the molecular mechanism in various biological processes but also help reveal the progression of tumor development.<sup>90</sup> Yan's team designed EGFR aptamers modified with Cy3 fluorescent dye as imager probes and then visualized the interaction between EGF and EGFR using dSTORM imaging at the single-molecule level.<sup>9</sup> The super-resolution images showed that EGFR formed protein clusters of different sizes on the COS-7 cell membrane. After adding EGF, the larger EGFR clusters were detected on the cellular membrane. These observations proved that the interaction between EGF and EGFR significantly influences the EGFR clustering pattern. Accordingly, visualization of protein organization can provide mechanistic insights into the interaction between biomolecules. Based on traditional PAINT



technology, Schueder et al. developed a technique for *in situ* proximity detection between two molecules with super-resolution readout ability and called it proximity-PAINT (pPAINT).<sup>91</sup> Specifically, the author constructed two different linear DNA probes as docking strands that are conjugated to antibodies to target  $\alpha$ -tubulin and  $\beta$ -tubulin, respectively. The imager probes consisted of two regions that complement the end sequences of the two docking strands. When two target proteins did not exhibit spatial proximity, a single docking strand could not be stably combined with the imager probes, resulting in no detectable fluorescence signal (Figure 7A,B). However, when  $\alpha$ -tubulin and  $\beta$ -tubulin were in close proximity, they generated  $\alpha$ - and  $\beta$ -tubulin heterodimers. The two docking strands would spatially colocalize and stably combine with the imager probes, detecting a distinct binding signal (Figure 7C). The development of this technique not only contributes to the study of the interaction between proteins but also can be further extended to realize the visualization of the interaction between other biomolecules.

In addition, nucleic acid probe-based SMLM can further explore the influence of complex cellular environments on intermolecular interactions. Chen et al. imaged protein tyrosine kinase-7 (PTK7) on MCF10A cell membrane based on aptamer probes and the STORM technique.<sup>92</sup> Then, the authors explored the effects of three cell membrane compositions (lipid raft, actin cytoskeleton, and carbohydrate chains) on the interactions between PTK7 proteins. All three compositions of the cell membranes were found to affect the interaction between PTK7 on the MCF10A membranes, and the degree of influence is different for the MCF10A basal and apical membranes. For lipid rafts, they were related to the stability of the interaction between PTK7 proteins. As shown in Figure 7E, the distribution area and size of PTK7 clusters on the basal and apical membranes were significantly decreased under the condition of lipid raft destruction (when the lipid raft was destroyed by *M $\beta$ CD*). As for actin cytoskeleton, Figure 7F shows the PTK7 clusters tended to form looser and larger protein domains when the actin cytoskeleton was depolymerized by cytochalasin B (CB) treatment. This suggested that actin cytoskeleton could promote protein interactions to form more compact protein clusters. Moreover, given that PTK7 was a glycoprotein, the authors further investigated how carbohydrate chains influence the interactions between PTK7 proteins. The results showed that with the destruction of carbohydrate chain structure by adding *N*-acetyl- $\beta$ -D-glucosaminidase (NAG), the average cluster area of PTK7 clusters on both the apical and basal membranes was smaller than that on normal membranes. Compared with the basal membrane, the PTK7 clusters were more affected on the apical membrane (Figure 7G). The author speculated that this may be because the carbohydrate molecules on the apical membrane were more likely to be exposed to the external environment; therefore, they could better interact with related molecules and ultimately affected the binding between PTK7.

In summary, SMLM imaging combined with nucleic acid probes of different conformations can realize the visualization of intracellular molecular interactions at subcellular resolution. In addition, this technique is able to further explore the key factors that affect intermolecular interactions, providing a molecular basis for a comprehensive understanding of cellular life activities.

## 5. SUMMARY AND OUTLOOK

In summary, although the development of SMLM imaging based on nucleic acid probes does not have a long history, the SMLM technique based on nucleic acid probes has shown great imaging potential. This technique not only provides a new tool for analyzing various cellular biomolecules but also opens up an emerging method for studying complex cell behavior. In this review, we mainly focus on the design of nucleic acid probes with different conformations used in SMLM technology and summarize the application of nucleic acid probe-based SMLM in intracellular biomolecular imaging. Adjusting the conformation of nucleic acid probes can optimize the SMLM imaging quality, enabling the visualization of the spatial distribution and interaction of cellular biomolecules at subdiffraction resolution. Although precise visualization via nucleic acid probe-based SMLM can broaden our understanding of various cell behaviors, there are still many problems that need to be solved. First, SMLM is the imaging technology with the highest spatial resolution among the existing super-resolution microscopy techniques. However, the processes of image acquisition and location reconstruction in SMLM imaging are very time-consuming, resulting in the inability to meet the requirements of high temporal and spatial resolutions simultaneously. This undoubtedly hinders the further development of the SMLM technique in the dynamic visualization of biomolecules. Second, for single-molecule imaging of intracellular biomolecules, nucleic acid probes need the ability to penetrate cell membranes and subcellular structures. This puts forward higher requirements for the size and specificity of the probes, restricting the diversity of probe design. Third, the current imaging depth of the SMLM technique is limited, making it difficult to perform super-resolution imaging of thick samples. Finally, nucleic acid probes are mainly applied in STORM and DNA-PAINT technology, but they are rarely used in PALM. In the future, the blinking rate, fluorescent signal, and size of nucleic acid probes need to be further optimized, aiming at better analyzing the fine structure and distribution of cellular biomolecules. In short, the nucleic acid probe-based SMLM imaging provides a universal platform not only for elucidating the molecular mechanisms of various life activities but also for guiding the diagnosis, treatment, and prognosis of diseases.

## AUTHOR INFORMATION

### Corresponding Authors

**Jie Tan** – Molecular Science and Biomedicine Laboratory (MBL), State Key Laboratory of Chemo/Biosensing and Chemometrics, College of Chemistry and Chemical Engineering, Hunan University, Changsha 410082, China; [orcid.org/0000-0002-0909-2904](https://orcid.org/0000-0002-0909-2904); Email: [tanjie0416@hnu.edu.cn](mailto:tanjie0416@hnu.edu.cn)

**Quan Yuan** – Molecular Science and Biomedicine Laboratory (MBL), State Key Laboratory of Chemo/Biosensing and Chemometrics, College of Chemistry and Chemical Engineering, Hunan University, Changsha 410082, China; [orcid.org/0000-0002-3085-431X](https://orcid.org/0000-0002-3085-431X); Email: [yanquan@whu.edu.cn](mailto:yanquan@whu.edu.cn)

### Authors

**Junyuan Wei** – Molecular Science and Biomedicine Laboratory (MBL), State Key Laboratory of Chemo/Biosensing and

Chemometrics, College of Chemistry and Chemical Engineering, Hunan University, Changsha 410082, China  
**Cailing Ji** – Molecular Science and Biomedicine Laboratory (MBL), State Key Laboratory of Chemo/Biosensing and Chemometrics, College of Chemistry and Chemical Engineering, Hunan University, Changsha 410082, China  
**Yingfei Wang** – Molecular Science and Biomedicine Laboratory (MBL), State Key Laboratory of Chemo/Biosensing and Chemometrics, College of Chemistry and Chemical Engineering, Hunan University, Changsha 410082, China

**Weihong Tan** – Molecular Science and Biomedicine Laboratory (MBL), State Key Laboratory of Chemo/Biosensing and Chemometrics, College of Chemistry and Chemical Engineering, Hunan University, Changsha 410082, China; [orcid.org/0000-0002-8066-1524](https://orcid.org/0000-0002-8066-1524)

Complete contact information is available at:  
<https://pubs.acs.org/10.1021/cbmi.3c00012>

### Author Contributions

<sup>§</sup>J. Wei and C. Ji contributed equally to this work.

### Notes

The authors declare no competing financial interest.

### ACKNOWLEDGMENTS

This work was supported by the Natural Science Foundation of Hunan Province (2022JJ20005), National Natural Science Foundation of China (22174038, 21925401, and 52221001), and Tencent Foundation.

### VOCABULARY

**PALM:** A super-resolution fluorescence microscopy technique based on the photoactivation method. Super-resolution imaging can be achieved by repeating the “activation–excitation–localization–bleaching” process many times; **STORM:** A super-resolution microscopy imaging technology with a resolution more than 10 times higher than that of a traditional optical microscope. The imaging principle is similar to PALM, but the fluorescent labels used are different; **dSTORM:** An improved technology based on STORM. This technique does not require the design of probes, but it uses fluorescent dyes that can realize the optical switch conversion by themselves. Other experimental processes of dSTORM are basically the same as STORM and can achieve the same imaging resolution; **PAINT:** A method for subdiffraction imaging that accumulates points by collisional flux. In PAINT imaging, the imaging target is continuously targeted by fluorescent probes in the solution. Each frame records the single-molecule fluorescence emitted by the nonspecific interaction between the freely diffused fluorescent probe and the target surface. The super-resolution images of target molecules were obtained by superposition of multiple collected images; **DNA-PAINT:** A multichannel super-resolution fluorescence imaging method based on association and dissociation of DNA strands. The oligonucleotide strand bound to the target (docking strand) repeatedly associates and dissociates with the complementary oligonucleotide strand coupled to the fluorescent dyes (imager probe). The instantaneous combination of the imager probe with the docking strand produces distinct blinking. By locating these blinking signals, the super-resolution image can be recon-

structed; **Aptamer:** Single-stranded oligonucleotides are generated by an in vitro evolution method known as systematic evolution of ligands by exponential enrichment (SELEX), capable of folding into specific three-dimensional structures to bind to their targets with superior specificity and affinity; **Black hole quencher:** A fluorescence quencher group that avoids the background residue common to other fluorescence quenchers, such as TAMRA, by combining FRET with the static quencher effect

### REFERENCES

- (1) Khater, I. M.; Nabi, I. R.; Hamarneh, G. A Review of Super-Resolution Single-Molecule Localization Microscopy Cluster Analysis and Quantification Methods. *Patterns (N Y)* **2020**, *1*, 100038.
- (2) Kikuchi, K.; Adair, L. D.; Lin, J.; New, E. J.; Kaur, A. Photochemical Mechanisms of Fluorophores Employed in Single-Molecule Localization Microscopy. *Angew. Chem., Int. Ed.* **2023**, *62*, e202204745.
- (3) Jimenez, A.; Friedl, K.; Leterrier, C. About samples, giving examples: Optimized Single Molecule Localization Microscopy. *Methods* **2020**, *174*, 100–114.
- (4) Vangindertael, J.; Camacho, R.; Sempels, W.; Mizuno, H.; Dedecker, P.; Janssen, K. P. F. An introduction to optical super-resolution microscopy for the adventurous biologist. *Methods Appl. Fluoresc.* **2018**, *6*, No. 022003.
- (5) Laxman, P.; Ansari, S.; Gaus, K.; Goyette, J. The Benefits of Unnatural Amino Acid Incorporation as Protein Labels for Single Molecule Localization Microscopy. *Front. Chem.* **2021**, *9*, 641355.
- (6) Yan, R.; Moon, S.; Kenny, S. J.; Xu, K. Spectrally Resolved and Functional Super-resolution Microscopy via Ultrahigh-Throughput Single-Molecule Spectroscopy. *Acc. Chem. Res.* **2018**, *51*, 697–705.
- (7) Samanta, S.; Gong, W.; Li, W.; Sharma, A.; Shim, I.; Zhang, W.; Das, P.; Pan, W.; Liu, L.; Yang, Z.; Qu, J.; Kim, J. S. Organic fluorescent probes for stochastic optical reconstruction microscopy (STORM): Recent highlights and future possibilities. *Coord. Chem. Rev.* **2019**, *380*, 17–34.
- (8) Yan, Q.; Cai, M.; Jing, Y.; Li, H.; Xu, H.; Sun, J.; Gao, J.; Wang, H. Quantitatively mapping the interaction of HER2 and EGFR on cell membranes with peptide probes. *Nanoscale* **2021**, *13*, 17629–17637.
- (9) Yan, Q.; Cai, M.; Zhou, L.; Xu, H.; Shi, Y.; Sun, J.; Jiang, J.; Gao, J.; Wang, H. Using an RNA aptamer probe for super-resolution imaging of native EGFR. *Nanoscale Adv.* **2019**, *1*, 291–298.
- (10) Wen, Y.; Li, L.; Wang, L.; Xu, L.; Liang, W.; Ren, S.; Liu, G. Biomedical Applications of DNA-Nanomaterials Based on Metallic Nanoparticles and DNA Self-Assembled Nanostructures. *Chin. J. Chem.* **2016**, *34*, 283–290.
- (11) Liu, M.; Xi, L.; Tan, T.; Jin, L.; Wang, Z.; He, N. A novel aptamer-based histochemistry assay for specific diagnosis of clinical breast cancer tissues. *Chin. Chem. Lett.* **2021**, *32*, 1726–1730.
- (12) Lu, B.; Deng, Y.; Peng, Y.; Huang, Y.; Ma, J.; Li, G. Fabrication of a Polyvalent Aptamer Network on an Electrode Surface for Capture and Analysis of Circulating Tumor Cells. *Anal. Chem.* **2022**, *94*, 12822–12827.
- (13) Wang, D. X.; Wang, J.; Wang, Y. X.; Du, Y. C.; Huang, Y.; Tang, A. N.; Cui, Y. X.; Kong, D. M. DNA nanostructure-based nucleic acid probes: construction and biological applications. *Chem. Sci.* **2021**, *12*, 7602–7622.
- (14) Krissanaprasit, A.; Key, C. M.; Pontula, S.; LaBean, T. H. Self-Assembling Nucleic Acid Nanostructures Functionalized with Aptamers. *Chem. Rev.* **2021**, *121*, 13797–13868.
- (15) Lai, Q.; Chen, W.; Zhang, Y.; Liu, Z. Application strategies of peptide nucleic acids toward electrochemical nucleic acid sensors. *Analyst* **2021**, *146*, 5822–5835.
- (16) Zhang, H.; Zhou, L.; Zhu, Z.; Yang, C. Recent Progress in Aptamer-Based Functional Probes for Bioanalysis and Biomedicine. *Chem.—Eur. J.* **2016**, *22*, 9886–9900.

- (17) Xia, Y.; Zhang, R.; Wang, Z.; Tian, J.; Chen, X. Recent advances in high-performance fluorescent and bioluminescent RNA imaging probes. *Chem. Soc. Rev.* **2017**, *46*, 2824–2843.
- (18) Casciarano, P.; Comes, M. C.; Sebastiani, A.; Mencattini, A.; Loli Piccolomini, E.; Martinelli, E. DeepCELO for 2D single-molecule localization in fluorescence microscopy. *Bioinformatics* **2022**, *38*, 1411–1419.
- (19) Lelek, M.; Gyparaki, M. T.; Beliu, G.; Schueder, F.; Griffié, J.; Manley, S.; Jungmann, R.; Sauer, M.; Lakadamyali, M.; Zimmer, C. Single-molecule localization microscopy. *Nat. Rev. Methods Primers* **2021**, *1*, 39.
- (20) Abbe, E. Beiträge zur Theorie des Mikroskops und der mikroskopischen Wahrnehmung. *Archiv für Mikroskopische Anatomie* **1873**, *9*, 413–468.
- (21) Wu, Y.; Tschanz, A.; Krupnik, L.; Ries, J. Quantitative Data Analysis in Single-Molecule Localization Microscopy. *Trends Cell Biol.* **2020**, *30*, 837–851.
- (22) Paúr, M.; Stoklasa, B.; Hradil, Z.; Sánchez-Soto, L. L.; Rehacek, J. Achieving the ultimate optical resolution. *Optica* **2016**, *3*, 1144–1147.
- (23) Li, Y.; Li, C.; Hao, X.; Liu, X.; Kuang, C. Review and Prospect for Single Molecule Localization Microscopy. *Laser Optoelectron. Prog.* **2020**, *57*, 240002.
- (24) Lin, D.-Y.; Qu, J.-L. Recent progress on super-resolution imaging and correlative super-resolution microscopy. *Acta Phys. Sin.* **2017**, *66*, 148703.
- (25) Kuznetsova, Y.; Neumann, A.; Brueck, S. R. J. Imaging interferometric microscopy-approaching the linear systems limits of optical resolution. *Opt. Express* **2007**, *15* (11), 6651–6663.
- (26) Huszka, G.; Gijs, M. A. M. Super-resolution optical imaging: A comparison. *Micro and Nano Engineering* **2019**, *2*, 7–28.
- (27) Ram, S.; Ward, E. S.; Ober, R. J. Beyond Rayleigh's criterion: A resolution measure with application to single-molecule microscopy. *Proc. Natl. Acad. Sci. U.S.A.* **2006**, *103*, 4457–4462.
- (28) Li, Y.; Liu, X.; Li, B. Single-cell biomagnifier for optical nanoscopes and nanotweezers. *Light Sci. Appl.* **2019**, *8*, 61.
- (29) Ma, H.; Liu, Y. Super-resolution localization microscopy: Toward high throughput, high quality, and low cost. *APL Photonics* **2020**, *5*, No. 060902.
- (30) LV, Z.-J.; LU, J.-Z.; WU, Y.-Q.; CHEN, L.-Y. Introduction to Theories of Several Super-resolution Fluorescence Microscopy Methods and Recent Advance in The Field. *Prog. Biochem. Biophys.* **2009**, *36*, 1626–1634.
- (31) Yang, Z.; Dong, Y.; Zong, S.; Li, L.; Yang, K.; Wang, Z.; Zeng, H.; Cui, Y. Water-dispersed CsPbBr<sub>3</sub> nanocrystals for single molecule localization microscopy with high location accuracy for targeted bioimaging. *Nanoscale* **2022**, *14*, 6392–6401.
- (32) Horrocks, M. H.; Palayret, M.; Klenerman, D.; Lee, S. F. The changing point-spread function: single-molecule-based super-resolution imaging. *Histochem. Cell Biol.* **2014**, *141*, 577–585.
- (33) Etheridge, T. J.; Boulineau, R. L.; Herbert, A.; Watson, A. T.; Daigaku, Y.; Tucker, J.; George, S.; Jonsson, P.; Palayret, M.; Lando, D.; Laue, E.; Osborne, M. A.; Klenerman, D.; Lee, S. F.; Carr, A. M. Quantification of DNA-associated proteins inside eukaryotic cells using single-molecule localization microscopy. *Nucleic Acids Res.* **2014**, *42*, e146.
- (34) Andronov, L.; Genthial, R.; Hentsch, D.; Klaholz, B. P. splitSMLM, a spectral demixing method for high-precision multi-color localization microscopy applied to nuclear pore complexes. *Commun. Biol.* **2022**, *5*, 1100.
- (35) Zhang, M.; Gao, J.; Chen, J.; Cai, M.; Jiang, J.; Tian, Z.; Wang, H. Enhanced dSTORM imaging using fluorophores interacting with cucurbituril. *Sci. China Chem.* **2016**, *59*, 848–852.
- (36) Jradi, F. M.; Lavis, L. D. Chemistry of Photosensitive Fluorophores for Single-Molecule Localization Microscopy. *ACS Chem. Biol.* **2019**, *14*, 1077–1090.
- (37) Pan, W.; Li, W.; Qu, J.; Ye, Y.; Qu, J.; Yang, Z. Research Progress on Organic Fluorescent Probes for Single Molecule Localization Microscopy. *Chin. J. Chem.* **2019**, *36*, 269–281.
- (38) Chen, C.; Zong, S.; Wang, Z.; Lu, J.; Zhu, D.; Zhang, Y.; Cui, Y. Imaging and Intracellular Tracking of Cancer-Derived Exosomes Using Single-Molecule Localization-Based Super-Resolution Microscope. *ACS Appl. Mater. Interfaces* **2016**, *8*, 25825–25833.
- (39) Betzig, E.; Patterson, G. H.; Sougrat, R.; Lindwasser, O. W.; Olenych, S.; Bonifacino, J. S.; Davidson, M. W.; Lippincott-Schwartz, J.; Hess, H. F. Imaging Intracellular Fluorescent Proteins at Nanometer Resolution. *Science* **2006**, *313*, 1642–1645.
- (40) Almada, P.; Culley, S.; Henriques, R. PALM and STORM: Into large fields and high-throughput microscopy with sCMOS detectors. *Methods* **2015**, *88*, 109–121.
- (41) Poole, J. J. A.; Mostaco-Guidolin, L. B. Optical Microscopy and the Extracellular Matrix Structure: A Review. *Cells* **2021**, *10*, 1760.
- (42) von Diezmann, L.; Shechtman, Y.; Moerner, W. E. Three-Dimensional Localization of Single Molecules for Super-Resolution Imaging and Single-Particle Tracking. *Chem. Rev.* **2017**, *117*, 7244–7275.
- (43) Rust, M. J.; Bates, M.; Zhuang, X. Sub-diffraction-limit imaging by stochastic optical reconstruction microscopy (STORM). *Nat. Methods* **2006**, *3*, 793–795.
- (44) Heilemann, M.; van de Linde, S.; Schuttpelz, M.; Kasper, R.; Seefeldt, B.; Mukherjee, A.; Tinnefeld, P.; Sauer, M. Subdiffraction-resolution fluorescence imaging with conventional fluorescent probes. *Angew. Chem., Int. Ed.* **2008**, *47*, 6172–6176.
- (45) van Wee, R.; Filius, M.; Joo, C. Completing the canvas: advances and challenges for DNA-PAINT super-resolution imaging. *Trends Biochem. Sci.* **2021**, *46*, 918–930.
- (46) Sharonov, A.; Hochstrasser, R. M. Wide-field subdiffraction imaging by accumulated binding of diffusing probes. *Proc. Natl. Acad. Sci. U.S.A.* **2006**, *103*, 18911–18916.
- (47) Schnitzbauer, J.; Strauss, M. T.; Schlichthaerle, T.; Schueder, F.; Jungmann, R. Super-resolution microscopy with DNA-PAINT. *Nat. Protoc.* **2017**, *12*, 1198–1228.
- (48) Guo, Y.; Gao, Y.; Liu, X.; Sun, H.; Shi, M.; Li, J.; Liu, Z.; Li, K. Screening and Specificity Analysis of Aptamer in Infiltrating Ductal Carcinoma of Breast. *ChemistrySelect* **2022**, *7*, e202200070.
- (49) Zhang, T.; Tian, T.; Lin, Y. Functionalizing Framework Nucleic-Acid-Based Nanostructures for Biomedical Application. *Adv. Mater.* **2022**, *34*, 2107820.
- (50) Jia, R.; Wang, T.; Jiang, Q.; Wang, Z.; Song, C.; Ding, B. Self-Assembled DNA Nanostructures for Drug Delivery. *Chin. J. Chem.* **2016**, *34*, 265–272.
- (51) Beliveau, B. J.; Boettiger, A. N.; Nir, G.; Bintu, B.; Yin, P.; Zhuang, X.; Wu, C. T. In Situ Super-Resolution Imaging of Genomic DNA with OligoSTORM and OligoDNA-PAINT. *Methods Mol. Biol.* **2017**, *1663*, 231–252.
- (52) Xie, L.; Dong, P.; Chen, X.; Hsieh, T. S.; Banala, S.; De Marzio, M.; English, B. P.; Qi, Y.; Jung, S. K.; Kieffer-Kwon, K. R.; Legant, W. R.; Hansen, A. S.; Schulmann, A.; Casellas, R.; Zhang, B.; Betzig, E.; Lavis, L. D.; Chang, H. Y.; Tjian, R.; Liu, Z. 3D ATAC-PALM: super-resolution imaging of the accessible genome. *Nat. Methods* **2020**, *17*, 430–436.
- (53) Konc, J.; Brown, L.; Whiten, D. R.; Zuo, Y.; Ravn, P.; Klenerman, D.; Bernardes, G. J. L. A Platform for Site-Specific DNA-Antibody Bioconjugation by Using Benzoylacrylic-Labelled Oligonucleotides. *Angew. Chem., Int. Ed.* **2021**, *60*, 25905–25913.
- (54) Jang, S.; Kim, M.; Shim, S. H. Reductively Caged, Photoactivatable DNA-PAINT for High-Throughput Super-resolution Microscopy. *Angew. Chem., Int. Ed.* **2020**, *59*, 11758–11762.
- (55) Chung, K. K. H.; Zhang, Z.; Kidd, P.; Zhang, Y.; Williams, N. D.; Rollins, B.; Yang, Y.; Lin, C.; Baddeley, D.; Bewersdorf, J. Fluorogenic DNA-PAINT for faster, low-background super-resolution imaging. *Nat. Methods* **2022**, *19*, 554–559.
- (56) Lee, J.; Park, S.; Kang, W.; Hohng, S. Accelerated super-resolution imaging with FRET-PAINT. *Mol. Brain* **2017**, *10*, 63.
- (57) Auer, A.; Strauss, M. T.; Schlichthaerle, T.; Jungmann, R. Fast, Background-Free DNA-PAINT Imaging Using FRET-Based Probes. *Nano Lett.* **2017**, *17*, 6428–6434.

- (58) Beliveau, B. J.; Boettiger, A. N.; Avendano, M. S.; Jungmann, R.; McCole, R. B.; Joyce, E. F.; Kim-Kiselak, C.; Bantignies, F.; Fonseka, C. Y.; Erceg, J.; Hannan, M. A.; Hoang, H. G.; Colognori, D.; Lee, J. T.; Shih, W. M.; Yin, P.; Zhuang, X.; Wu, C. T. Single-molecule super-resolution imaging of chromosomes and in situ haplotype visualization using Oligopaint FISH probes. *Nat. Commun.* **2015**, *6*, 7147.
- (59) Markey, F. B.; Parashar, V.; Batish, M. Methods for spatial and temporal imaging of the different steps involved in RNA processing at single-molecule resolution. *Wiley Interdiscip. Rev. RNA* **2021**, *12*, e1608.
- (60) Broude, N. E. Stem-loop oligonucleotides: a robust tool for molecular biology and biotechnology. *Trends Biotechnol.* **2002**, *20*, 249–256.
- (61) Melo, S. A.; Luecke, L. B.; Kahlert, C.; Fernandez, A. F.; Gammon, S. T.; Kaye, J.; LeBleu, V. S.; Mittendorf, E. A.; Weitz, J.; Rahbari, N.; Reissfelder, C.; Pilarsky, C.; Fraga, M. F.; Piwnicka-Worms, D.; Kalluri, R. Glypican-1 identifies cancer exosomes and detects early pancreatic cancer. *Nature* **2015**, *523*, 177–182.
- (62) Yang, F.; Ning, Z.; Ma, L.; Liu, W.; Shao, C.; Shu, Y.; Shen, H. Exosomal miRNAs and miRNA dysregulation in cancer-associated fibroblasts. *Mol. Cancer* **2017**, *16*, 148.
- (63) Chen, C.; Zong, S.; Wang, Z.; Lu, J.; Zhu, D.; Zhang, Y.; Zhang, R.; Cui, Y. Visualization and intracellular dynamic tracking of exosomes and exosomal miRNAs using single molecule localization microscopy. *Nanoscale* **2018**, *10*, S154–S162.
- (64) Ni, Y.; Cao, B.; Ma, T.; Niu, G.; Huo, Y.; Huang, J.; Chen, D.; Liu, Y.; Yu, B.; Zhang, M. Q.; Niu, H. Super-resolution imaging of a 2.5 kb non-repetitive DNA in situ in the nuclear genome using molecular beacon probes. *Elife* **2017**, *6*, e21660.
- (65) Pereira, P. M.; Gustafsson, N.; Marsh, M.; Mhlanga, M. M.; Henriques, R. Super-beacons: Open-source probes with spontaneous tuneable blinking compatible with live-cell super-resolution microscopy. *Traffic* **2020**, *21*, 375–385.
- (66) Qi, H.; Xu, Y.; Hu, P.; Yao, C.; Yang, D. Construction and applications of DNA-based nanomaterials in cancer therapy. *Chin. Chem. Lett.* **2022**, *33*, 1131–1140.
- (67) Meng, H. M.; Liu, H.; Kuai, H.; Peng, R.; Mo, L.; Zhang, X. B. Aptamer-integrated DNA nanostructures for biosensing, bioimaging and cancer therapy. *Chem. Soc. Rev.* **2016**, *45*, 2583–2602.
- (68) Dai, Z.; Xie, X.; Gao, Z.; Li, Q. DNA-PAINT Super-Resolution Imaging for Characterization of Nucleic Acid Nanostructures. *ChemPlusChem.* **2022**, *87*, e202200127.
- (69) Yang, F.; Li, Q.; Wang, L.; Zhang, G. J.; Fan, C. Framework-Nucleic-Acid-Enabled Biosensor Development. *ACS Sens.* **2018**, *3*, 903–919.
- (70) Scheible, M. B.; Ong, L. L.; Woehrstein, J. B.; Jungmann, R.; Yin, P.; Simmel, F. C. A Compact DNA Cube with Side Length 10 nm. *Small* **2015**, *11*, S200–S205.
- (71) Lin, C.; Jungmann, R.; Leifer, A. M.; Li, C.; Levner, D.; Church, G. M.; Shih, W. M.; Yin, P. Submicrometre geometrically encoded fluorescent barcodes self-assembled from DNA. *Nat. Chem.* **2012**, *4*, 832–839.
- (72) Zancchi, F. C.; Manzo, C.; Alvarez, A. S.; Derr, N. D.; Garcia-Parajo, M. F.; Lakadamyali, M. A DNA origami platform for quantifying protein copy number in super-resolution. *Nat. Methods* **2017**, *14*, 789–792.
- (73) Liu, Z.; Zheng, Y.; Xie, T.; Chen, Z.; Huang, Z.; Ye, Z.; Xiao, Y. Clickable rhodamine spirolactam based spontaneously blinking probe for super-resolution imaging. *Chin. Chem. Lett.* **2021**, *32*, 3862–3864.
- (74) Panchapakesan, S. S.; Jeng, S. C.; Unrau, P. J. RNA complex purification using high-affinity fluorescent RNA aptamer tags. *Ann. N.Y. Acad. Sci.* **2015**, *1341*, 149–155.
- (75) Biomarkers Definitions Working Group. Biomarkers and surrogate endpoints: preferred definitions and conceptual framework. *Clin. Pharmacol. Ther.* **2001**, *69*, 89–95.
- (76) Mischak, H.; Allmaier, G.; Apweiler, R.; Attwood, T.; Baumann, M.; Benigni, A.; Bennett, S. E.; Bischoff, R.; Bongcam-Rudloff, E.; Capasso, G.; Coon, J. J.; D’Haese, P.; Dominiczak, A. F.; Dakna, M.; Dihazi, H.; Ehrich, J. H.; Fernandez-Llama, P.; Fliser, D.; Frokiaer, J.; Garin, J.; Girolami, M.; Hancock, W. S.; Haubitz, M.; Hochstrasser, D.; Holman, R. R.; Ioannidis, J. P. A.; Jankowski, J.; Julian, B. A.; Klein, J. B.; Kolch, W.; Luider, T.; Massy, Z.; Mattes, W. B.; Molina, F.; Monsarrat, B.; Novak, J.; Peter, K.; Rossing, P.; Sánchez-Carbayo, M.; Schanstra, J. P.; Semmes, O. J.; Spasovski, G.; Theodorescu, D.; Thongboonkerd, V.; Vanholder, R.; Veenstra, T. D.; Weissinger, E.; Yamamoto, T.; Vlahou, A. Recommendations for Biomarker Identification and Qualification in Clinical Proteomics. *Sci. Transl. Med.* **2010**, *2*, 46ps42.
- (77) Cheng, X.; Yin, W. Probing Biosensing Interfaces With Single Molecule Localization Microscopy (SMLM). *Front. Chem.* **2021**, *9*, 655324.
- (78) Schlichthaerle, T.; Eklund, A. S.; Schueder, F.; Strauss, M. T.; Tiede, C.; Curd, A.; Ries, J.; Peckham, M.; Tomlinson, D. C.; Jungmann, R. Site-Specific Labeling of Affimers for DNA-PAINT Microscopy. *Angew. Chem., Int. Ed.* **2018**, *57*, 11060–11063.
- (79) Doyle, L. M.; Wang, M. Z. Overview of Extracellular Vesicles, Their Origin, Composition, Purpose, and Methods for Exosome Isolation and Analysis. *Cells* **2019**, *8*, 727.
- (80) Ciesla, M.; Skrzypek, K.; Kozakowska, M.; Loboda, A.; Jozkowicz, A.; Dulak, J. MicroRNAs as biomarkers of disease onset. *Anal. Bioanal. Chem.* **2011**, *401*, 2051–2061.
- (81) Tomasetti, M.; Lee, W.; Santarelli, L.; Neuzil, J. Exosome-derived microRNAs in cancer metabolism: possible implications in cancer diagnostics and therapy. *Exp. Mol. Med.* **2017**, *49*, e285.
- (82) Delcanale, P.; Porciani, D.; Pujals, S.; Jurkevich, A.; Chetrusca, A.; Tawiah, K. D.; Burke, D. H.; Albertazzi, L. Aptamers with Tunable Affinity Enable Single-Molecule Tracking and Localization of Membrane Receptors on Living Cancer Cells. *Angew. Chem., Int. Ed.* **2020**, *59*, 18546–18555.
- (83) Schueder, F.; Lara-Gutiérrez, J.; Haas, D.; Beckwith, K. S.; Yin, P.; Ellenberg, J.; Jungmann, R. Super-Resolution Spatial Proximity Detection with Proximity-PAINT. *Angew. Chem., Int. Ed.* **2021**, *60*, 716–720.
- (84) Ferhan, A. R.; Jackman, J. A.; Cho, N. J. Integration of Quartz Crystal Microbalance-Dissipation and Reflection-Mode Localized Surface Plasmon Resonance Sensors for Biomacromolecular Interaction Analysis. *Anal. Chem.* **2016**, *88*, 12524–12531.
- (85) Hellman, L. M.; Fried, M. G. Electrophoretic mobility shift assay (EMSA) for detecting protein-nucleic acid interactions. *Nat. Protoc.* **2007**, *2*, 1849–1861.
- (86) Homocianu, M.; Airinei, A. Intra-/inter-molecular interactions – Identification and evaluation by optical spectral data in solution. *J. Mol. Liq.* **2017**, *225*, 869–876.
- (87) Kabiri, M.; Unsworth, L. D. Application of isothermal titration calorimetry for characterizing thermodynamic parameters of biomolecular interactions: peptide self-assembly and protein adsorption case studies. *Biomacromolecules* **2014**, *15*, 3463–3473.
- (88) Qian, X.; LeVe, C. M.; Freeman, J. K.; Dougall, W. C.; Greene, M. I. Heterodimerization of epidermal growth factor receptor and wild-type or kinase-deficient Neu: a mechanism of interreceptor kinase activation and transphosphorylation. *Proc. Natl. Acad. Sci. U.S.A.* **1994**, *91*, 1500–1504.
- (89) Plattner, C.; Hackl, H. Modeling therapy resistance via the EGFR signaling pathway. *FEBS J.* **2019**, *286*, 1284–1286.
- (90) Deng, W.; Gu, L.; Li, X.; Zheng, J.; Zhang, Y.; Duan, B.; Cui, J.; Dong, J.; Du, J. CD24 associates with EGFR and supports EGF/EGFR signaling via RhoA in gastric cancer cells. *J. Transl. Med.* **2016**, *14*, 32.
- (91) Schueder, F.; Lara-Gutiérrez, J.; Haas, D.; Beckwith, K. S.; Yin, P.; Ellenberg, J.; Jungmann, R. Super-Resolution Spatial Proximity Detection with Proximity-PAINT. *Angew. Chem., Int. Ed.* **2021**, *60*, 716–720.
- (92) Chen, J.; Li, H.; Wu, Q.; Yan, Q.; Sun, J.; Liang, F.; Liu, Y.; Wang, H. Organization of Protein Tyrosine Kinase-7 on Cell Membranes Characterized by Aptamer Probe-Based STORM Imaging. *Anal. Chem.* **2021**, *93*, 936–945.